

We are IntechOpen, the world's leading publisher of Open Access books Built by scientists, for scientists

6,900

Open access books available

186,000

International authors and editors

200M

Downloads

Our authors are among the

154

Countries delivered to

TOP 1%

most cited scientists

12.2%

Contributors from top 500 universities



WEB OF SCIENCE™

Selection of our books indexed in the Book Citation Index
in Web of Science™ Core Collection (BKCI)

Interested in publishing with us?
Contact book.department@intechopen.com

Numbers displayed above are based on latest data collected.
For more information visit www.intechopen.com



Oxidation Chemistry of Metal(II) Salen-Type Complexes

Yuichi Shimazaki

Additional information is available at the end of the chapter

<http://dx.doi.org/10.5772/48372>

1. Introduction

The oxidation chemistry of metal complexes has been widely developed in recent years, affording deep insights into the reaction mechanisms for many useful homogeneous catalytic reactions and enzymatic reactions at the active site of metalloenzymes [1]. In the course of the studies, a large number of novel complexes have been synthesized and well characterized [2-18], and especially high valent metal complexes formed as a result of redox reactions have become important in catalytic and biological systems. In general high valent metal complexes have been meant to show the complexes oxidized at the metal center, and the formal oxidation state is identical with the oxidation state of the central metal ion reported in [19-23]. For example, one-electron oxidation of potassium hexacyanoferrate(II), $K_4[Fe(CN)_6]$, gives potassium hexacyanoferrate(III), $K_3[Fe(CN)_6]$, whose valence state of the central iron ion is +III and agrees with the experimental valence state of the ion. In contrast to this, the formal oxidation number of the central metal ion of the complexes of iminophenolate dianion, $(L^{AP})^{2-}$ is not always identical with the experimental valence state reported in references [24,25]. In the case of $[Ni(L^{AP})_2]^0$, the formal oxidation state of the central nickel ion is +IV, but the experimental valence state of nickel can be assigned to be +II, and two iminophenolate dianions are oxidized to iminosemiquinonate radical anions $(L^{SQ})^-$ (**Figure 1**).

Such a difference between the formal oxidation number and the experimental oxidation state is also observed in biological systems. Recently, it has been reported that various radicals can be generated at a proximal position of the metal center in metalloproteins, and the radical can sometimes interact with the central metal ion as shown in reference [21]. Galactose oxidase (GO) is a single copper oxidase, which catalyzes a two-electron oxidation of a primary alcohol to the corresponding aldehyde [21-24]. The active site structure of the inactive form of GO is shown in **Figure 2**, where two imidazole rings of histidine residues,

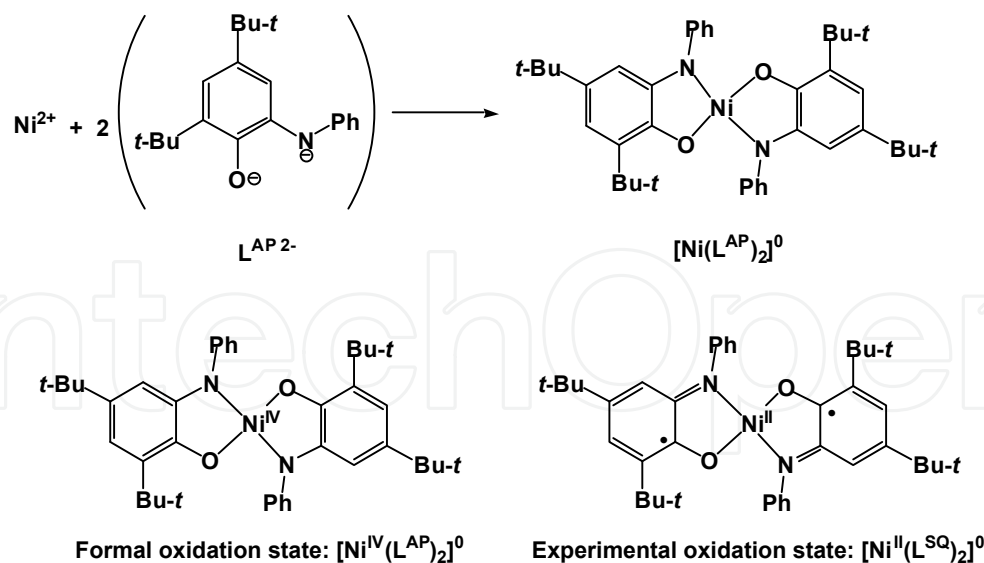


Figure 1. An example showing the difference between the experimental oxidation state and the formal oxidation number in the Ni complexes of iminophenolate dianions, $[\text{Ni}(\text{L}^{\text{AP}})_2]^0$.

two phenol moieties of tyrosine residues, and an acetate ion are coordinated to the copper(II) ion [24]. One of two phenol moieties is in the deprotonated form and is coordinated to the copper ion at an equatorial position, and another phenol moiety is protonated and located at an apical position.

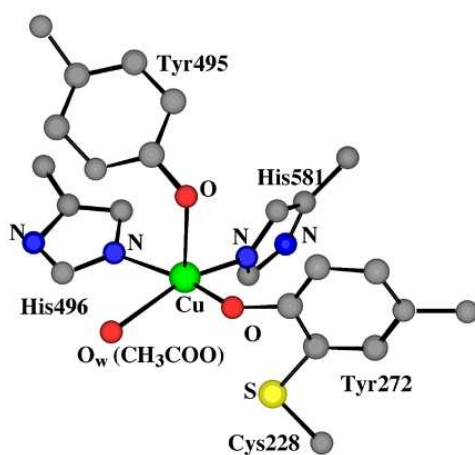
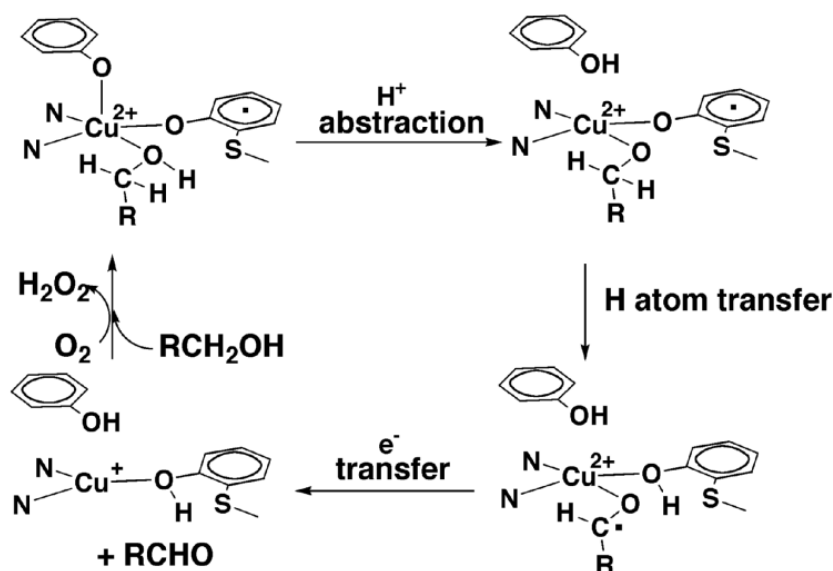


Figure 2. Active site structure of the inactive form of GO.

Conversion to the active form of GO occurs upon one-electron oxidation and deprotonation from the apical phenol moiety, which gives the structure with the two phenolate moieties coordinated to the copper center. This active form should act as a two-electron oxidant, causing the conversion from primary alcohol to aldehyde. Therefore, the formal oxidation state of the active form of GO can be described as a Cu(III)-phenolate species. Actually, the active form of GO had been considered to be a copper(III) species [25,26], but early in 1990's, various spectroscopic studies of the active form of GO revealed the formation of the phenoxyl radical species and the Cu(II)-phenoxyl radical bond. The free phenoxyl radical is very unstable with half life estimated to be 2.4 ms at ambient conditions, while the Cu(II)-

phenoxyl radical in the active form of GO has a long life; the radical is not quenched for more than one week at room temperature [22,23,27,28]. Thus, properties of the metal coordinated phenoxyl radical show a significant change from those of the free phenoxyl radical.

The proposed reaction mechanism of GO is that the primary alcohol is coordinated to the Cu(II)-phenoxyl radical species generated by molecular oxygen and oxidized by an intramolecular two-electron redox reaction with the hydrogen atom scission from the alcohol moiety to give the aldehyde and the Cu(I)-phenol species (**Scheme 1**) reported in [22,23]. The Cu(I)-phenol complex is oxidized by molecular oxygen to regenerate the Cu(II)-phenoxyl radical species.



Scheme 1. Proposed mechanism of galactose oxidase (GO).

For understanding the detailed mechanism of GO and the properties of the metal complexes with the coordinated phenoxyl radical, many metal-phenolate complexes have been synthesized, and their oxidation behavior and properties of the oxidized forms have been characterized in [12,13, 29-36]. Salen (Salen = di(salicylidene)ethylenediamine) and its family are one of the most important and famous ligands having two phenol moieties (**Figure 3**) [37,38]. One of the characteristics of Salen is its preference for a square planar 2N2O coordination environment, while the distortion from the square plane can be introduced by changing the diamine backbone. A number of metal-Salen complexes have been reported to be the very important catalysts for oxidation and conversion of various organic substrates from early 1990's [37]. While studies on oxidative reaction intermediates are in progress, the oxidation state of the metal ions in the active species has not been fully understood until now. Detailed descriptions of the oxidation state of the intermediate are sometimes complicated, because the oxidation locus on oxidized metal complexes is often different from the "formal" oxidation site [19,20]. Although "formal" and "experimental" oxidation numbers are identical in many cases, they are often used as synonyms, since the term of the physical or experimental oxidation state has not been accepted in some areas of chemistry.

The present argument is focused on recent advances in the chemistry related with the synthesis, characterization, and reactivity of some of the one-electron oxidized metal(II)–salen type complexes, especially the complexes of group 10 metal(II) ions, Ni(II), Pd(II), and Pt(II) [39-43], and Cu(II) complexes [44-47] (**Figure 3**).

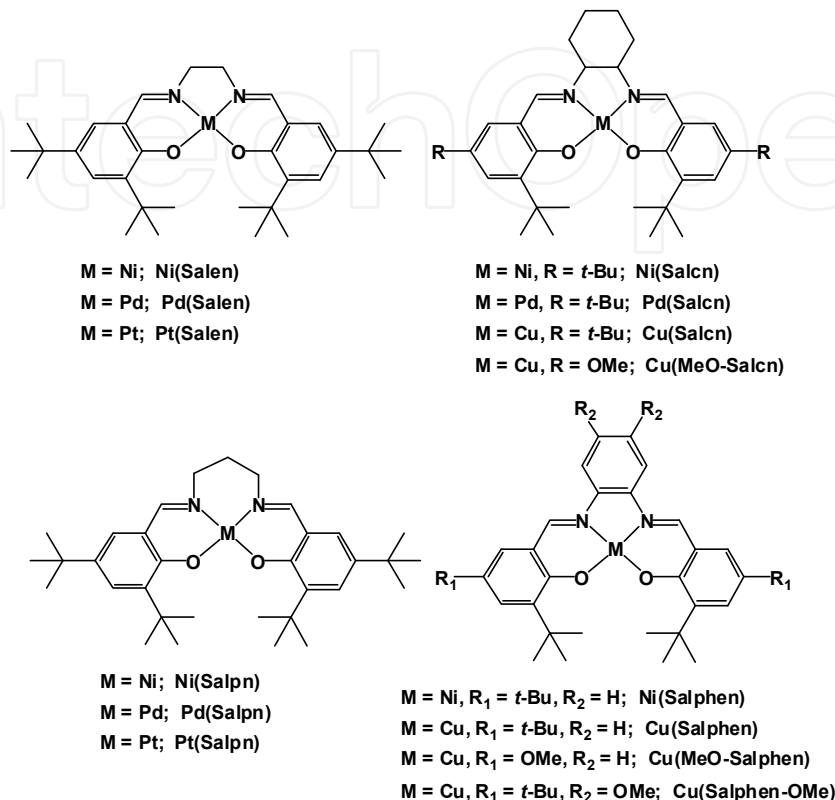


Figure 3. Abbreviations of salen-type complexes.

Various useful and interesting salen-type complexes have been synthesized and characterized until now [48], and detailed electronic structural studies have recently been reported for a dinuclear chelating salen-type ligand having a catechol and a tetra(amino)tri(hydroxy)phenyl moiety [49, 50]. In view of the interest in the redox properties of metal-phenolate complexes, detailed electronic structures of the one-electron oxidized complexes are discussed in order to understand the electronic structure difference between the metal-centered and ligand-centered oxidation products and its dependence on the properties of metal ions and substituents of the phenolate moiety. For this reason, this argument is described only for a few examples whose detailed electronic structures have been clarified.

2. Redox potentials of phenol and metal(II) salen-type complexes

One-electron oxidation of closed-shell organic molecules is generally difficult, and the one-electron oxidized products may be unstable. Oxidation of the free phenol similarly gives the unstable phenoxyl radical described in the introduction and references [21-23,27,28]. The potential of formation of the phenoxyl radical is predicted to be high, and actually the

potential of a tri(*tert*-butyl)phenol was estimated to be +1.07 V as reported in [51]. On the other hand, the oxidation potential of the phenolate anion is much lower (-0.68 V) in comparison with that of phenol [52], suggesting that deprotonation from phenol is favorable for formation of the free radical .

The oxidation chemistry of metal phenolate complexes has shown that the oxidation potentials of phenolate complexes are intermediate between those of free phenolate and free phenol [53]. Such a trend is also applied to the salen-type complexes, and most of the Cu(II) and group 10 metal(II) salen-type complexes exhibited two reversible redox waves in the range of 0 to 1.5 V vs NHE, due to having two phenolate moieties [29-31, 39-47]. On the other hand, the metal centered one- and two-electron oxidized complexes may possibly be generated in the similar potential range. Some copper(III) [12,13] and nickel(III) [54,55] complexes have been reported, and two-electron oxidized species of the group 10 metal ions, especially some Pd(IV) and Pt(IV) complexes, have been reported. Some of the metal complexes such as K_2PdCl_6 and K_2PtCl_6 are commercially available [56]. Therefore, the experimental oxidation state can not be determined from the oxidation potential only. The redox potentials of some salen-type complexes are listed in **Table 1**, and the voltammograms of two copper(II) complexes are shown as examples in **Figure 4** [39-47].

complex	potential (E / V vs. Fc / Fc ⁺)	complex	potential (E / V vs. Fc / Fc ⁺)
Ni(Salcn)	0.46, 0.80	Ni(Salphen)	0.58, 0.80
Pd(Salcn)	0.45, 0.80	Cu(Salcn)	0.45, 0.65
Pt(Salen)	0.35, 0.94	Cu(MeO-Salcn)	0.28, 0.44
Ni(Salp _n)	0.43, 0.69	Cu(Salphen)	0.65, 0.83
Pd(Salp _n)	0.52, 0.88	Cu(MeO-Salphen)	0.38, 0.49
Pt(Salp _n)	0.44, 0.99	Cu(Salphen-OMe)	0.41, 0.70

Table 1. Redox potential of Cu(II) and group 10 metal complexes

From the list of **Table 1**, the ranges of both first and second redox potentials are relatively narrow, especially the range of the first redox potentials being from 0.28 to 0.65 V. Such a narrow range may be generally ascribed to the fact that the all the complexes have a similar oxidation locus. The small potential differences are due to the substitution of the phenolate moiety and the ligand structure. However, there are some different electronic structures among the one-electron oxidized forms of the complexes in Table 1, i.e., a M^{III}-phenolate ground state complex, a M^{II}-phenoxyl radical where the radical electron is fully delocalized on two phenolate moieties, a relatively localized M^{II}(phenolate)(phenoxyl) complex, and a M^{II}(dinitrogen ligand radical)(phenolate)₂ species [39-47]. The similarity of the potentials indicates that formation of all of the oxidized species is due to a simple electron transfer without significant structural changes. Thus, the experimental oxidation state of the oxidized complexes cannot be determined only from the redox potentials.

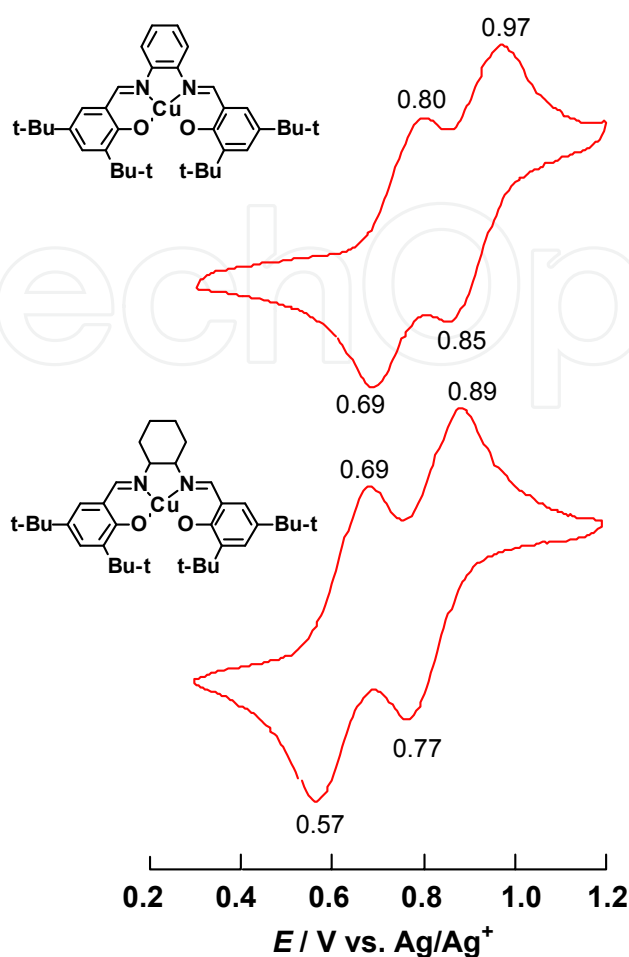


Figure 4. Cyclic voltammograms of Cu(II) complexes: Top, Cu(Salphen); bottom, Cu(Salcn).

3. Isolation and solid state characterization of one-electron oxidized complexes

One-electron oxidized complexes have been synthesized by reaction with a one-electron oxidant, such as Ce^{IV} , Ag^{I} , NO^+ , some organic reagents, and so on [57]. For most complexes shown in **Figure 3**, one-electron oxidized species were generated by addition of AgSbF_6 to the CH_2Cl_2 solution of metal(II) salen-type complexes. Ag^{I} with a potential of 0.799 V vs. NHE can act as a one-electron oxidant for complexes [57,58]. The oxidation method using Ag ion is useful for generation of the relatively stable oxidized complexes, since Ag^0 is an easily removable product formed in the course of the oxidation. Some solutions of one-electron oxidized complexes were kept standing for a few days to give the products as crystals.

The X-ray crystal structure analyses of one-electron oxidized group 10 metal salen-type complexes are shown in **Figure 5** [41-43]. The structures of all these complexes were found to be similar to those of the corresponding complexes before oxidation, which supports the CV results that significant structure changes did not occur in the course of the oxidation.

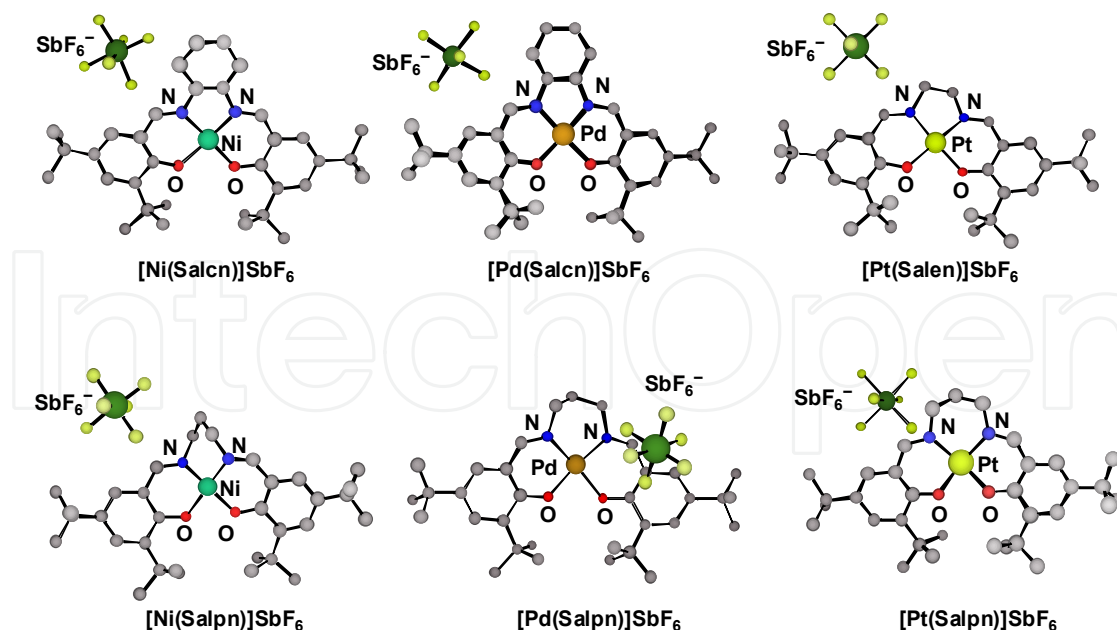
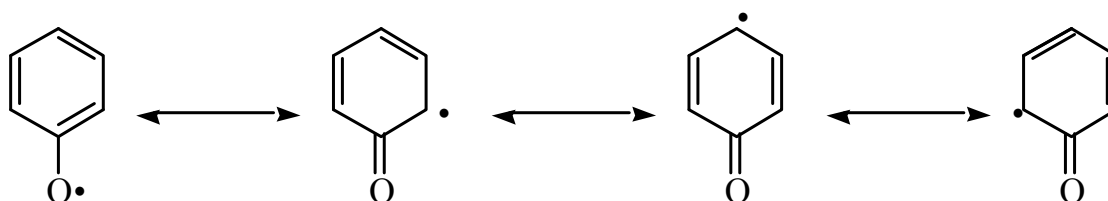


Figure 5. Crystal structures of one-electron oxidized group 10 metal salen-type complexes

However, a close look into the details of the crystal structures reveals that there are subtle differences between them, and especially the oxidized Pd(II) complexes are different from the other complexes [42,43]. Comparison of the 5-membered dinitrogen chelate backbones of the Salcn and Salen complexes indicates that upon oxidation the Ni and Pt complexes exhibited a clear coordination sphere contraction due to shortening of the M–O and M–N bond lengths. On the other hand, the Pd complex showed an unsymmetrical contraction [42]: One of the Pd–O bonds (2.003 Å) is longer than the other (1.963 Å), and the C–O bond (1.263 Å) of the phenolate moiety with the longer Pd–O bond is shorter than the other C–O bond (1.317 Å). The phenolate moiety with a shorter C–O bond length has the lengthening of the ring *ortho* C–C bonds in comparison with those of the other one. These structural features of the phenolate moiety in the oxidized Pd complex are in good agreement with the characteristics of the phenoxyl radical, which showed the quinoid form due to delocalization of the radical electron on the phenolate moiety as shown in **Scheme 2** and reference [53]. Such properties were also detected for the Pd complex with the 6-membered dinitrogen chelate back bone, [Pd(Salpn)]SbF₆ [43]. In addition, the SbF₆[−] counterion was positioned close to the quinoid moiety of this complex; the closest distance between the SbF₆[−] and the C–O carbon atom of the phenoxyl ligand was 3.026 Å. Therefore, one-electron oxidized Pd(II) complexes can be assigned to relatively localized Pd^{II}(phenoxyl)(phenolate) complexes.



Scheme 2. Canonical forms of the phenoxyl radical

The Ni and Pt 5-membered dinitrogen chelate complexes also exhibited a clear symmetrical coordination sphere contraction in both two M–O and two M–N bond lengths (ca. 0.02 Å) upon oxidation, and the C–O bond distances of these complexes are also shorter than the same bonds before oxidation [41,43]. These observations suggest that the complexes have the phenoxyl radical characteristics and that the radical electron is delocalized on the two phenolate moieties. Indeed, the XPS and K-edge XANES of an oxidized Ni complex showed the same binding energies and pre-edge peak of nickel ion as those of the complex before oxidation [40]. These results supported that the valence state of the nickel ion is +II. In the case of Pt complexes, the XPS of the oxidized complex was slightly different from that before oxidation. The binding energies of the Pt ion in the oxidized complex were +0.2 eV higher, and L_{III}-edge XANES exhibited an increasing white line [59]. Such spectral features suggest that the oxidation state of the Pt ion in the oxidized complex is higher than +II but that the differences are rather small [40]. Therefore, [Pt(Salen)]SbF₆ can be described mainly as the Pt(II)-phenoxyl radical species, but the radical electron is fully delocalized over the whole molecule including the central metal ion [40]. On the other hand, the six-membered Ni^{II} and Pt^{II} Salpn chelate complexes are slightly different from the 5-membered dinitrogen chelate Salcn and Salen complexes [43]. Crystal structures of both oxidized Salpn complexes exhibited two crystallographically independent molecules in the unit cells. The M–O and M–N bond lengths do not differ substantially between the two molecules in the unit cell. The bond lengths in the coordination plane are ca. 0.02 Å shorter than those of the neutral complexes, and this contraction upon oxidation is in good agreement with the 5-membered dinitrogen chelate complexes. However, the C–O bond lengths of the two phenolate moieties differed for the two independent molecules; one of the molecules showed very similar C–O bond lengths, while the bond lengths in the other molecule were slightly different, showing a similar tendency to that of the oxidized Pd complexes. Therefore, the 6-membered Ni and Pt chelate complexes can be considered to be closer to the localized phenoxyl radical metal(II) complexes in comparison with the 5-membered chelate complex, Salcn and Salpn due to the chelate effect of the dinitrogen backbone [43]. However, determination of the detailed electronic structure of oxidized salen-type complexes, especially 5-membered Ni and Pt chelate complexes, only from the X-ray crystal structure analysis may be difficult, since we can detect mainly the contraction of the coordination sphere, which is predicted to be also observed in high valent metal salen-type complexes.

On the other hand, the electronic structure determination of the Cu complexes are clearly made by X-ray structure analyses. Structures of three one-electron oxidized Cu^{II} salen-type complexes are shown in **Figure 6** [44,45,47]. X-ray analyses of all these complexes established that their structures are similar to those before oxidation, indicating a simple one-electron transfer from these precursors. However, the three Cu complexes have different electronic structures.

Figure 6 shows that the oxidized Cu(II) complexes have the SbF₆[−] counterion at different positions. The structures of the same dinitrogen backbone complexes, [Cu(Salcn)]SbF₆ and [Cu(MeO-Salcn)]SbF₆, indicate that a weak axial Cu–F interaction (2.76 Å) exists between the counterion and the metal center in [Cu(Salcn)]⁺ [45], whereas [Cu(MeO-Salcn)]⁺ has a weak

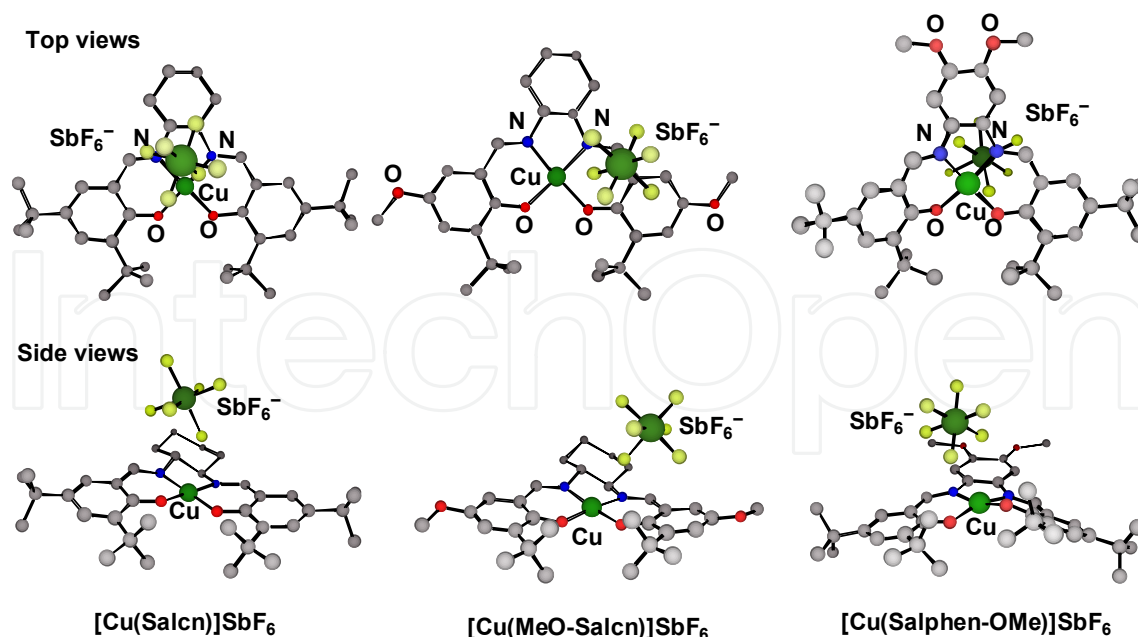


Figure 6. Crystal structures of one-electron oxidized Cu(II) salen-type complexes

F–C interaction between the counterion and one side of the phenolate moieties [44]. This difference suggests that the oxidation locus of these complexes are different; [Cu(Salcn)]SbF₆ has a Cu(III) character, while [Cu(MeO-Salcn)]SbF₆ is a Cu(II)-phenoxyl radical complex. [Cu(Salcn)]SbF₆ showed contraction of the coordination sphere without shortening of the C–O bonds of both phenolate moieties and distortion of the coordination plane was substantially reduced from that in Cu(Salcn) [45]. Such structural features are in good agreement with those of the low-spin d⁸ Cu(III) complexes [12,13]. Indeed, the XAF and XPS studies of [Cu(Salcn)]SbF₆ reported the Cu(III)-phenolate ground state, because the pre-edge of oxidized complex was more than 1 eV higher, and the binding energies of Cu ion in the oxidized complex was also 1 eV higher as compared with the neutral complex Cu(Salcn) [45]. These characteristics are in good agreement with the Cu(III) valence state [12,13]. On the other hand, the MeO-substituted complex [Cu(MeO-Salcn)]SbF₆ exhibits that the C–O bond of one-side of the phenolate moieties is shortened and that the Cu–O bond with the shortened phenolate moiety becomes longer [44]. The counterion is close to the phenolate moiety of the shortened C–O bond. Such characteristics are in good agreement with those of the oxidized Pd(Salpn) having a relatively localized Pd^{II}(phenoxyl)(phenolate) structure. Therefore, [Cu(MeO-Salcn)]SbF₆ can be described as a localized Cu^{II}(phenoxyl)(phenolate) complex [44].

Another one-electron oxidized complex, [Cu(Salphen-OMe)]SbF₆, has a different electronic structure from the previous two Salcn complexes [47]. The C–C and C–O bond lengths within the phenolate rings do not differ significantly from those of the complex before oxidation, Cu(Salphen-OMe). Although there is only a slight contraction of the Cu–O and Cu–N bonds, the copper ion geometry is significantly distorted toward a tetrahedral geometry in our case (the dihedral angle of 22° between the O1–Cu–N1 and O2–Cu–N2 planes). These structural features indicate that the oxidation locus of [Cu(Salphen-OMe)]⁺ is

neither the two phenolates nor the central copper ion. A striking feature upon oxidation is the change in the bond lengths within the phenyl ring. Further the counterion SbF_6^- is located close to the *o*-phenylenediamine moiety. Therefore, the oxidized complex, $[\text{Cu}(\text{Salphen-OMe})]\text{SbF}_6$, can be assigned to the Cu(II)-diiminobenzene radical species [47]. In this connection, the one-electron oxidized complex without any substitution on the *o*-phenylenediamine moiety, $[\text{Cu}(\text{Salphen})]^+$, has a different electronic structure, which corresponds to the Cu(II)-phenoxy radical species [46]. The methoxy substitution in the phenyl ring leads to a different electronic structure due to its electron donating property.

4. Magnetic properties of one-electron oxidized metal salen-type complexes

The behavior of the phenoxy radical bound to metal ions with an open-shell configuration such as Cu(II) having the d^9 configuration is different from that bound to Cu(III) ground state complex, $[\text{Cu}(\text{Salcn})]\text{SbF}_6$. In general, Cu(III) complexes have a square-planar geometry and are diamagnetic and EPR silent due to the low-spin d^8 configuration [12,13]. The Cu(II)-phenoxy radical complex, on the other hand, has two electron spins on different nuclei, and therefore the spin-spin interaction should be considered in [29-31]. In the case of the oxidized Cu(II) salen-type complexes, since correlation between ligand *p*-orbital and the copper $d_{x^2-y^2}$ orbital having an unpaired electron is close to orthogonal, the *d*-electron spin of copper ion coupled with radical electron spin ferromagnetically [60].

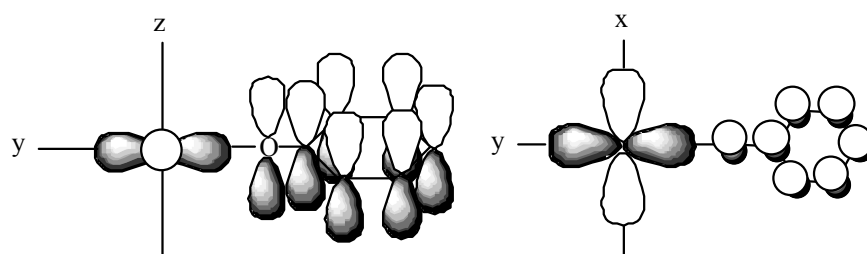


Figure 7. Schematic view of the orthogonality between ligand *p*-orbital and the copper $d_{x^2-y^2}$ orbital

Magnetic properties of $[\text{Cu}(\text{Salcn})]\text{SbF}_6$ in the solid state have been reported to be a temperature independent diamagnetic species with the effective magnetic moment $m_{\text{eff}} = 0.3 m_{\text{B.M.}}$ at 300 K, which is in good agreement with the considerations from the crystal structure analysis²⁵. On the other hand, the EPR spectra of the phenoxy radical complex, $[\text{Cu}(\text{MeO-Salcn})]\text{SbF}_6$, were silent in the temperature range of 4–100 K, which may be due to the large ZFS parameters ($D > 0.3 \text{ cm}^{-1}$) reported in [44]. The expression “EPR silent” does not specify the detailed electronic structure of the oxidized Cu(II)-phenolate complex, since it could refer to any of the cases, antiferromagnetism, ferromagnetism, and diamagnetism [61]. However, DFT calculation revealed that the two SOMOs consist of the $d_{x^2-y^2}$ orbital of copper ion and the ligand *p*-orbital, which are situated in the orthogonal positions. Therefore, magnetic properties of this complex can be assigned to the $S = 1$ ground state with ZFS parameters $D = 0.722 \text{ cm}^{-1}$ and $E/D = 0.150$ based on the *ab initio* calculation [44]. Cu(II)-diiminobenzene radical complex, $[\text{Cu}(\text{Salphen-OMe})]\text{SbF}_6$, is predicted to be ferromagnetic

$S = 1$ ground state due to similar orthogonality between radical and copper d orbitals. Indeed, $[\text{Cu}(\text{Salphen-OMe})]\text{SbF}_6$ can be assigned to the ferromagnetic species with $S = 1$ ground state, based on the pulse EPR experiment [47].

On the other hand, ligand oxidation and metal oxidation can be distinguished in one-electron oxidation of the group 10 metal salen-type complexes. One-electron oxidized group 10 metal salen-type complexes have an unpaired electron with $S = 1/2$. Metal-centered oxidation species show a large g value and large anisotropy due to coupling with the metal nuclear spin, while the radical species show a g value close to 1.998 for free electron. The EPR spectra of the oxidized Ni(II) salen-type complexes are shown in **Figure 8**, and those of the oxidized group 10 metal Salpn complexes are shown in **Figure 9** and references [40,41,43]. In the general case of low-spin d^7 Ni(III) complexes, the EPR spectrum shows the axial signals with $g_{\text{iso}} = \text{ca. } 2.15$ [54]. The spectrum of the one-electron oxidized Ni(Salcn) complex shows the signals at $g_{\text{av}} = 2.05$, which is different from the spectrum of the characteristic Ni(III) signals [39-41]. The g values of these oxidized Ni complexes supported formation of the Ni(II)-phenoxyl radical complex as the main species with some contribution from Ni(II) ion, which is in good agreement with the results of the solid state characterizations in [39,40]. Further, $[\text{Ni}(\text{Salpn})]^+$ showed the isotropic signal at $g = 2.04$. Lack of the hyperfine structures based on the nickel nuclear spin suggests that the contribution of the central nickel ion is rather small and that the radical electron is slightly localized on the ligand [43].

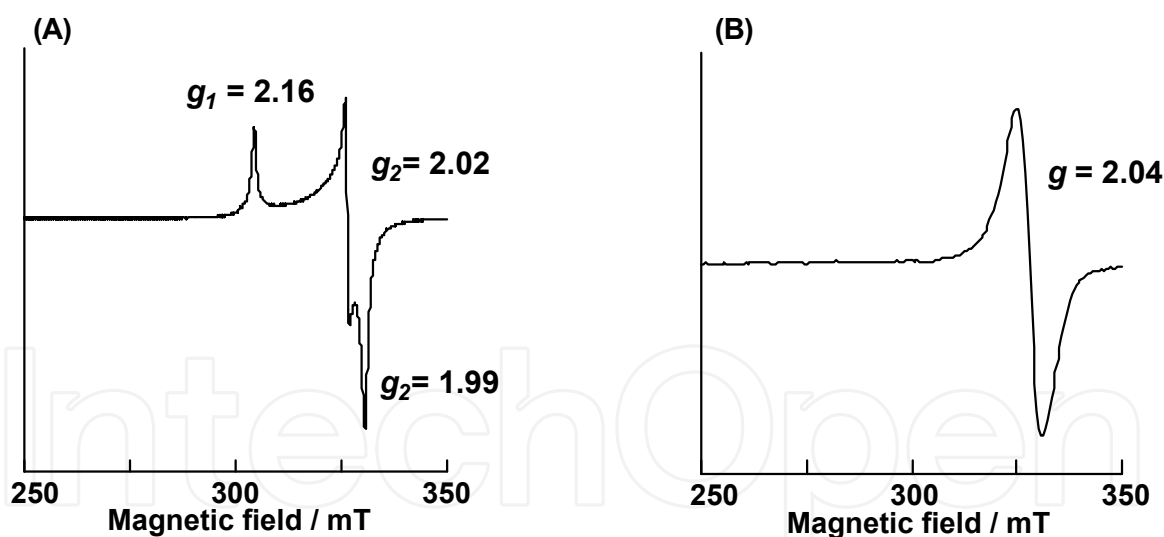


Figure 8. EPR spectra of oxidized Ni complexes in CH_2Cl_2 at 77 K ; (A) $[\text{Ni}(\text{Salcn})]^+$ and (B) $[\text{Ni}(\text{Salpn})]^+$.

Such a trend is also observed for the Pd and Pt complexes. The one-electron oxidized Pd complexes, $[\text{Pd}(\text{Salen})]^+$ and $[\text{Pd}(\text{Salpn})]^+$, have a similar characteristic; the band width of the signal is narrow, and the g value is close to the free electron value ($g = 2.010$ for $[\text{Pd}(\text{Salen})]^+$, and $g = 2.007$ for $[\text{Pd}(\text{Salpn})]^+$) in comparison with the other group 10 metal salen-type complexes. The results matches with the results of solid state characterization as relatively localized $\text{Pd}^{\text{II}}(\text{phenoxyl})(\text{phenolate})$ complexes [40,43]. However, only $[\text{Pd}(\text{Salcn})]^+$ shows the EPR signals coupled with Pd ion nuclear spin, indicating that the 6-membered

dinitrogen chelate complex has the spin more localized on the ligand [43]. On the other hand, one-electron oxidized Pt complexes, $[\text{Pt}(\text{Salen})]^+$ and $[\text{Pt}(\text{Salpn})]^+$, exhibited the g value similar to that of oxidized Ni complexes, while the band width is significantly large with rhombic component. Such the EPR spectral features are in good agreement with the considerations from the solid state characterization that the oxidized Pt complexes are mainly Pt^{II} -phenoxyl radical species but have a large distribution of the radical electron spin at the Pt ion [40,43].

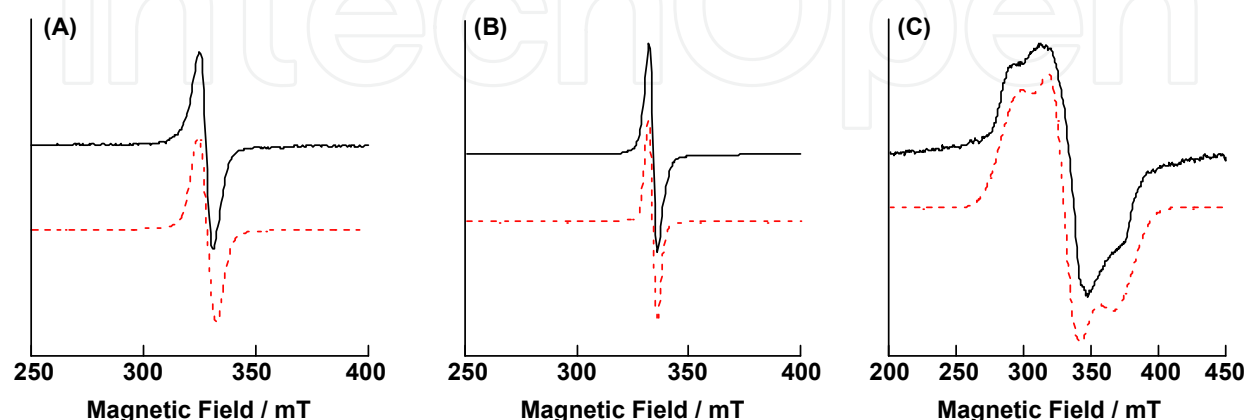


Figure 9. EPR spectra of oxidized group 10 metal Salpn complexes: (A) $[\text{Ni}(\text{Salpn})]^+$; (B) $[\text{Pd}(\text{Salpn})]^+$ and (C) $[\text{Pt}(\text{Salpn})]^+$. Black solid lines are measured spectra and red dashed lines are simulations of measurements.

5. Characterization of one-electron oxidized M(II) salen-type complexes in solution

The electronic structure of oxidized complexes in solution is sometimes different from that in the solid state, due to some additional factors such as interactions with solvent molecules and removal of restriction from the lattice energy. One of the important examples is shown for $[\text{Cu}(\text{Salcn})]\text{SbF}_6$ in [45]. This complex can be assigned to the $\text{Cu}(\text{III})$ -phenolate complex in the solid state described above, but in CH_2Cl_2 solution it is different. The absorption spectrum of $[\text{Cu}(\text{Salcn})]\text{SbF}_6$ exhibited two intense bands at 18600 and 5700 cm^{-1} in the visible and NIR region (**Figure 10**). These two bands were assigned by the time-dependent density functional theory calculation (TD-DFT) to the HOMO-4 to LUMO and the HOMO to LUMO transition, respectively [62]. The HOMOs mainly consist of the ligand molecular orbitals, while contribution of the copper d orbital to LUMO becomes higher. From the result, these two transitions are concluded to be the ligand-to-copper charge transfer (LMCT) bands [45]. However, the LMCT band intensity is temperature dependent, decreasing with increasing temperature (**Figure 10**, inset). Temperature dependent magnetic susceptibility change was also detected by NMR study, and the effective magnetic moment of the CD_2Cl_2 solution of $[\text{Cu}(\text{Salcn})]\text{SbF}_6$ increased with increasing temperature with 25 % triplet state at 178 K. These temperature dependent changes are reversible, and activation parameters can be estimated to be $\Delta H^\circ = 1.1 \pm 0.1 \text{ kcal mol}^{-1}$, $\Delta S^\circ = 3.5 \pm 0.1 \text{ cal K}^{-1} \text{ mol}^{-1}$, respectively (**Figure 11**). Therefore, the CH_2Cl_2 solution of $[\text{Cu}(\text{Salcn})]\text{SbF}_6$ showed the

valence tautomerism between Cu(III)-phenolate and Cu(II)-phenoxyl radical governed by temperature as reported in [45].

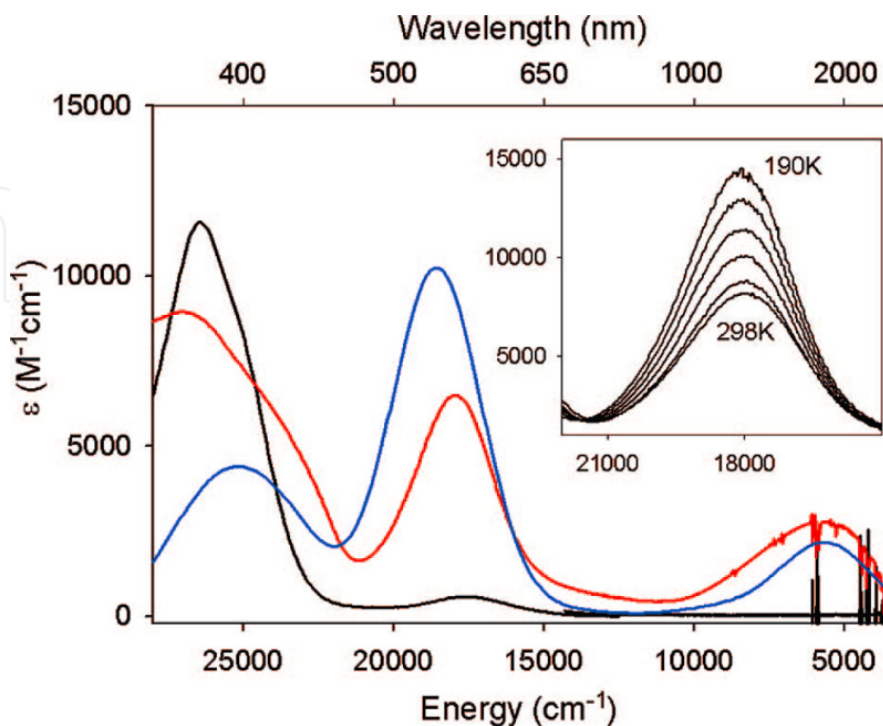


Figure 10. UV-vis-NIR spectra of 0.08 mM solutions of Cu(Salcn) (black) and [Cu(Salcn)]SbF₆ (red) in CH₂Cl₂, and the calculated spectrum for singlet [Cu(Salcn)]⁺ (blue). Inset: Temperature dependence (from 298 to 190 K) of the 18000-cm⁻¹ band.

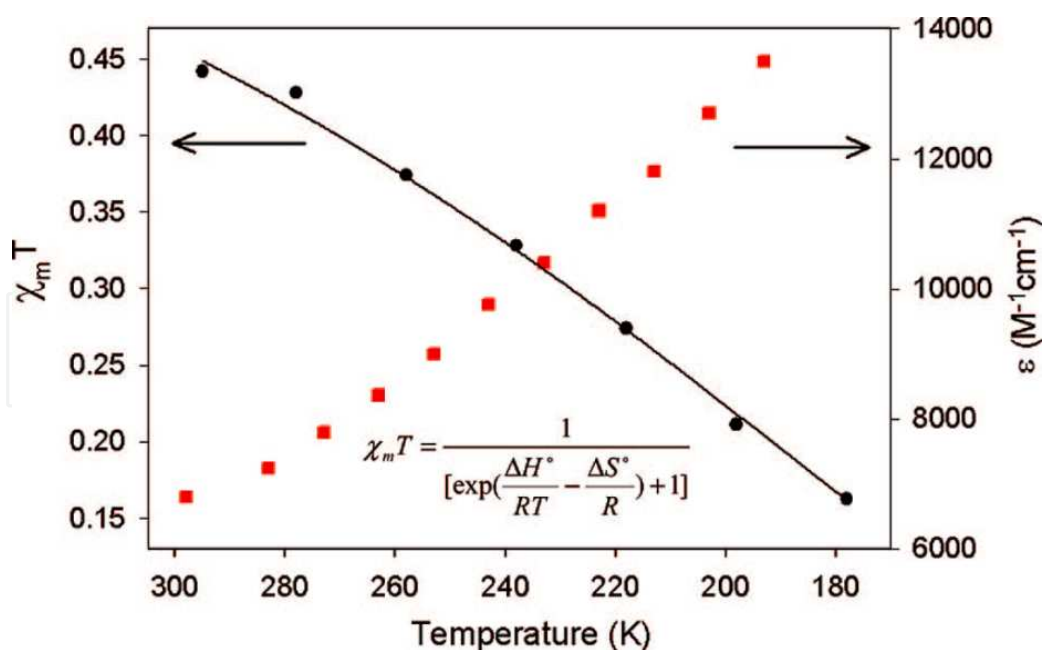


Figure 11. Comparison of the temperature dependent solution susceptibility by ¹H NMR (black circles, CD₂Cl₂) and 18000-cm⁻¹ band intensity (red squares, CH₂Cl₂) for [Cu(Salcn)]SbF₆. Fitting the susceptibility values (solid line) to the equation indicated affords thermodynamic parameters for the equilibrium.

One-electron oxidized Ni(Salcn) complexes also exhibit a valence state change. The one-electron oxidation of Ni(Salcn) in DMF caused a color change to purple, exhibiting a new absorption band at 476 nm. In CH₂Cl₂, however, a different UV-vis absorption spectrum was detected with the bands at 1100, 900 and 415(shoulder) nm (**Figure 12**) [39]. The CH₂Cl₂ solution showed an EPR signal similar to that of the solid sample, indicating the Ni(II)-phenoxyl radical species, while the DMF solution of the oxidized species showed the characteristic Ni(III) signals. The resonance Raman spectra of both solutions are different, the CH₂Cl₂ solution showed the phenoxyl radical ν_{7a} and ν_{8a} bands at 1504 and 1605 cm⁻¹, respectively [28], while the DMF solution showed only small shifts (3 cm⁻¹) of the phenolate ν_{11a} band at *ca.* 1530 cm⁻¹ [39]. The valence state difference dependent on solvents can be considered to be due to coordination of DMF molecules to the nickel ion. Addition of exogenous ligands such as pyridine to the CH₂Cl₂ solution of [Ni(Salcn)]⁺ causes the color change from green to purple, and the solution showed the UV-vis absorption spectrum and EPR signals characteristic of Ni(III) complexes [63,64]. Further, the X-ray crystal structure of μ -oxo Ni^{III}(salen) dimer has been reported to be synthesized by addition of excess O₂ under basic conditions (**Figure 13**) [55]. Such a valence state change by coordination of an exogenous ligand is also observed for the 6-membered chelate [Ni(Salpn)]⁺ but not detected for the other group 10 metal salen-type complexes [40,43].

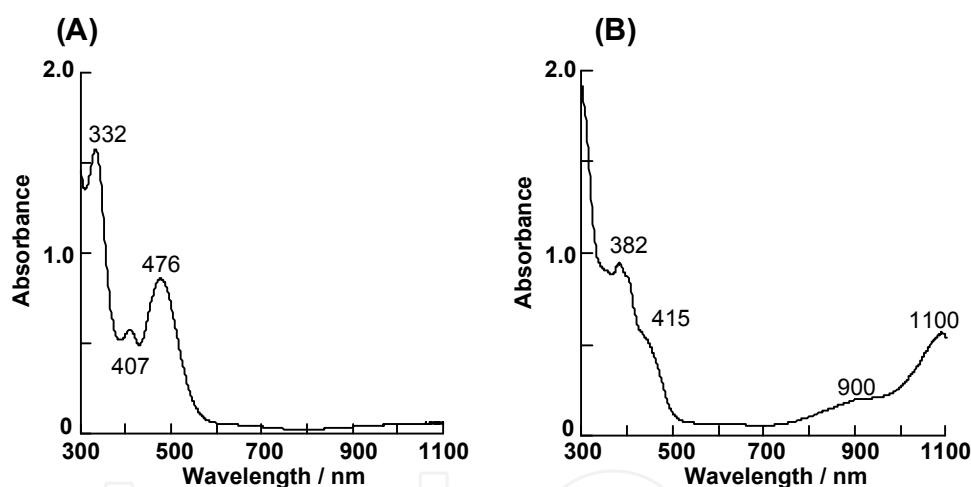


Figure 12. Absorption spectra of solutions of [Ni(Salcn)]SbF₆: (A) in DMF; (B) in CH₂Cl₂.

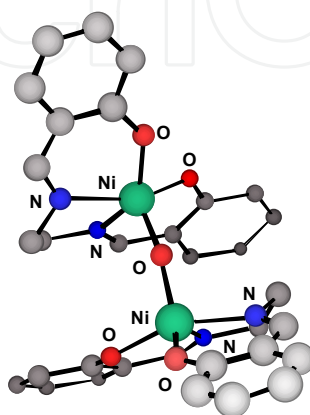


Figure 13. Crystal structure of [Ni(salen)]₂O.

One of the important characteristics of the oxidized group 10 metal salen-type complexes, $[M^{\text{II}}(\text{Salen})]^+$, $[M^{\text{II}}(\text{Salcn})]^+$, and $[M^{\text{II}}(\text{Salpn})]^+$, is the appearance of an intense NIR band at $\sim 5000\text{ cm}^{-1}$ [42,43]. The band is assigned to the phenolate to phenoxyl radical (ligand-to-ligand) charge transfer (LLCT) by TD-DFT calculation. The analyses of the low energy NIR LLCT band reveal the degree of the radical delocalization, which can be estimated by Robin-Day classification for understanding the mixed valence system. The classification is categorized in three systems as follows: (1) a fully localized system (class I), (2) a fully delocalized system (class III), and (3) a moderately coupled system (class II) [65]. In the case of the fully localized system, there is no characteristic LLCT band in the NIR region, while the fully delocalized system shows an intense NIR LLCT band. On the other hand, the moderate coupling system exhibits a less intense NIR band, which depends on small perturbations such as solvent polarity. UV-vis-NIR spectra of group 10 metal salen-type complexes are shown in **Figure 14** and reference [43].

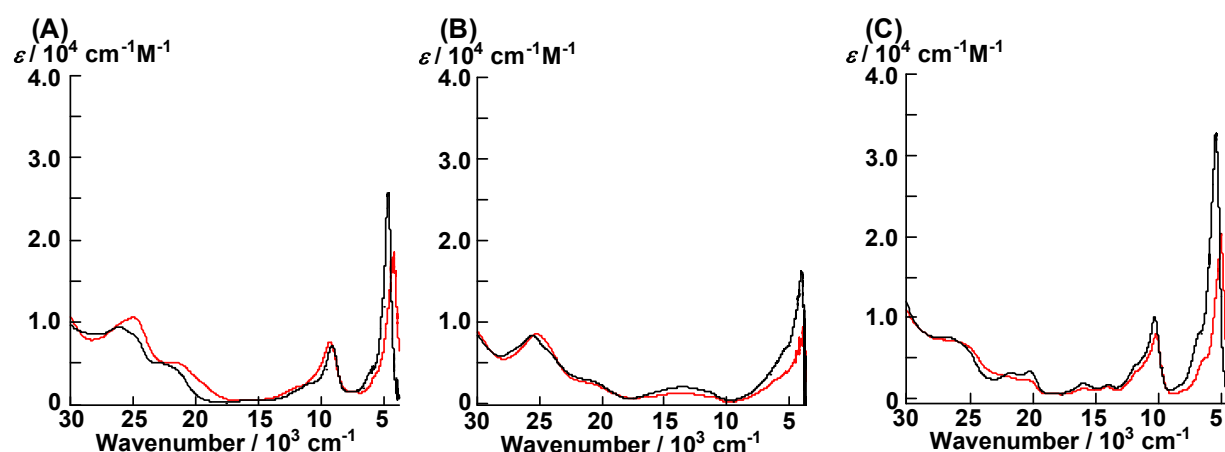


Figure 14. UV-vis-NIR spectra of the one-electron oxidized the group 10 metal salen-type complexes: Salpn complexes, black line; 5-membered chelate complexes, red line. (A) Ni complexes; (B) Pd complexes; (C) Pt complexes.

The NIR band intensity is in the order, $\text{Pt} > \text{Ni} > \text{Pd}$. The NIR spectrum of the oxidized Pd complex showed a less intense band in comparison to the bands of the oxidized Ni and Pt complexes, and the band was the most solvent dependent. From these results, the oxidized Pd complexes may be slightly closer to the class II moderately coupled system among the oxidized group 10 metal-salen type complexes, that is, the oxidized Pd complex is a more localized system [42]. On the other hand, the NIR band of the Pt complexes was the highest in intensity and less solvent dependent. These results strongly support that the Pt complexes belong to the class III delocalization system, which is also supported by all other experimental results in [42]. As compared with 5-membered and 6-membered chelate dinitrogen backbone complexes, intensity of all of the NIR bands of 6-membered complexes is decreased, indicating that the 6-membered dinitrogen chelate leads to radical localization on the ligand [43]. It is therefore obvious that there is a clear difference between the delocalized and localized systems of the phenoxyl radical species.

6. Conclusion

The oxidation chemistry of the group 10 metal(II) and copper(II) salen-type complexes is discussed in this chapter, to show that the oxidized salen-type complexes have a variety of the oxidation products. The CV of these salen-type complexes exhibited two reversible redox waves of one-electron process and the values of the first redox potential of complexes were in a narrow range. However, one-electron oxidized complexes have different electronic structures, which are dependent on the central metal ion, aromatic ring substituents, and the chelate effect of the dinitrogen backbone.

The electronic structure of the one-electron oxidized group 10 metal salen-type complexes is mainly a metal(II)-radical species, but there is a subtle difference in the detailed electronic structures. The oxidized nickel complexes are the delocalized phenoxyl radical species, but the valence state changes upon addition of an exogenous ligand to form the Ni(III)-phenolate species. Such a valence state change could not be detected for Pd and Pt complexes. The oxidized Pd complexes are relatively localized phenoxyl radical species, which can be described as the Pd(phenoxyl)(phenolate) complexes. On the other hand, the oxidized Pt(II) complexes are regarded as the fully delocalized phenoxyl radical species and have a large distribution of the radical electron spin on the central Pt ion. Among the group 10 metal complexes, the Pd complexes have the most localized electronic structure. The energy of the *d*-orbitals of group 10 M(II) ions increase in the order Pd < Ni < Pt, due to variation of the effective nuclear charge in combination with relativistic effects.

The one-electron oxidized complexes have different electronic structures showing at least three sorts of complexes described as M(III)-phenolate, M(II)-phenoxyl radical, and M(II)-ligand radical except the phenoxyl radical. These electronic structure differences give rise to the crystal structure differences, especially the position of the counterion in the proximity of the oxidation locus. The bond lengths and angles of oxidized complexes also reveal the electronic structure difference. The magnetic susceptibility, UV-vis-NIR measurements, and other physicochemical data substantiate the electronic structure difference and afford further insights into the novel properties, such as valence tautomerism between Cu(III)-phenolate and Cu(II)-phenoxyl radical in CH₂Cl₂ solution of oxidized Cu(Salcn) complex. It is now obvious that detailed electronic structures of one-electron oxidized complex should be concluded on the basis of the results of various physical measurements.

Many salen-type complexes have been reported also in organic chemistry as the catalysts for organic molecular conversion [17]. However, the detailed reaction mechanism has not been discussed, and especially the electronic structure of the catalyst has been unclear. Information on the detailed electronic structure of the metal ion in complexes may lead to construction of more efficient catalysts and discovery of further interesting phenomena.

Author details

Yuichi Shimazaki

College of Science, Ibaraki University, Bunkyo, Mito, Japan

Acknowledgement

The author is grateful to Prof. Dr. Osamu Yamauchi, Kansai University, for helpful comments and suggestions during preparation of this manuscript.

7. References

- [1] Holm R. H, Kennepohl P, Solomon E. I (1996) Structural and Functional Aspects of Metal Site in Biology. *Chem. Rev.* 96, 2239-2314.
- [2] Sono H, Roach M. P, Coulter E. D, Dawson J. H (1996) Structure and Reaction Mechanism in the Heme Dioxygenases. *Chem. Rev.* 96, 2841-2887.
- [3] Meunier B, de Visser S. P, Shaik S (2004) Theoretical Perspective on Structure and Mechanisms of Cytochrome P450 Enzymes. *Chem. Rev.* 104, 3947-3980.
- [4] Rohde J.-U, In J. H, Lim M. H, Brennessel W. W, Bukowski M. R, Stubna A, Münck E, Nam W, Que L. Jr (2003) Crystallographic and Spectroscopic Characterization of a Nonheme Fe(IV)=O Complex. *Science*, 299, 1037-1039.
- [5] Baik M, Newcomb M, Friesner R. A, Lippard S. J (2003) Insights into the P-to-Q conversion in the catalytic cycle of methane monooxygenase from a synthetic model system. *Chem. Rev.*, 2003, 103, 2385-2420.
- [6] Tshuva E. Y, Lippard S. J (2004) Synthetic models for non-heme carboxylate-bridged diiron metalloproteins: strategies and tactics. *Chem. Rev.* 104, 987-1012.
- [7] Costas M, Mehn M. P, Jensen M. P, Que L. Jr (2004) Dioxygen Activation at Mononuclear Nonheme Iron Active Sites: Enzymes, Models, and Intermediates. *Chem. Rev.* 104, 939-986.
- [8] Solomon E. I, Brunold T. C, Davis M. I, Kemsley J. N, Lee S.-K, Lehnert N, Neese F, Skulan A. J, Yang Y.-S, Zhou J (2000) Geometric and electronic structure/function correlations in non-heme iron enzymes. *Chem. Rev.* 100, 235-350.
- [9] Nam, W (2007) Special Issue on Dioxygen Activation by Metalloenzymes and Models *Acc. Chem. Res.* 40, 465-635.
- [10] Petrenko T, George S. D, Aliaga-Alcalde N, Bill E, Mienert B, Xiao Y, Guo Y, Sturhahn W, Cramer S. P, Wieghardt K, Neese F (2007) Characterization of a Genuine Iron(V)-Nitrido Species by Nuclear Resonant Vibrational Spectroscopy Coupled to Density Functional Calculations. *J. Am. Chem. Soc.* 129, 11053-11060.
- [11] Gunay A, Theopold K. H (2010) C-H Bond Activations by Metal Oxo Compounds. *Chem. Rev.* 110, 1060-1081.
- [12] Mirica L. M, Ottenwaelder X, Stack T. D. P (2004) Structure and Spectroscopy of Copper-Dioxygen Complexes. *Chem. Rev.* 104, 1013-1046.
- [13] Lewis E. A, Tolman W. B, (2004) Reactivity of Dioxygen-Copper Systems. *Chem. Rev.* 104, 1047-1076.
- [14] Jörgensen C. K (1969) *Oxidation Numbers and Oxidation States*. Heidelberg, Springer.
- [15] Chirik P. J, Wieghardt K (2010) Radical Ligands Confer Nobility on Base-Metal Catalysts. *Science* 327, 794-795.
- [16] Holland P. L (2008) Electronic Structure and Reactivity of Three-Coordinate Iron Complexes. *Acc. Chem. Res.* 41, 905-914.

- [17] de Bruin B, Hetterscheid D. G. H, Koekkoek A. J. J, Grützmacher H (2007) The Organometallic Chemistry of Rh, Ir, Pd and Pt based Radicals; Higher Valent Species. *Prog. Inorg. Chem.* 55, 247-253.
- [18] Kaim, W (2011) Manifestations of Noninnocent Ligand Behavior. *Inorg. Chem.* 50, 9752-9765.
- [19] Chaudhuri P, Verani C. N, Bill E, Bothe E, Weyhermüller T, Wieghardt K (2001) Electronic Structure of Bis(*o*-iminobenzosemiquinonato)metal Complexes (Cu, Ni, Pd). The Art of Establishing Physical Oxidation States in Transition-Metal Complexes Containing Radical Ligands. *J. Am. Chem. Soc.* 123, 2213-2223.
- [20] Herebian D, Bothe E, Bill E, Weyhermüller T, Wieghardt K (2001) Experimental Evidence for the Noninnocence of *o*-Aminothiophenolates: Coordination Chemistry of *o*-Iminothionebenzosemiquinonate(1-) π -Radicals with Ni(II), Pd(II), Pt(II). *J. Am. Chem. Soc.* 123, 10012-10023.
- [21] Stubbe J, van der Donk W. A, (1998) Protein Radicals in Enzyme Catalysis. *Chem. Rev.* 98, 705.
- [22] Whittaker J. W (1994) Radical copper oxidases. *Met. Ions Biol. Syst.* 30, 315-360.
- [23] Whittaker J. W (2003) Free radical catalysis by galactose oxidase. *Chem. Rev.* 103, 2347-2363.
- [24] Ito N, Phillips S. E. V, Yadav K. D. S, Knowles P. F (1994) Crystal structure of a free radical enzyme, galactose oxidase. *J. Mol. Biol.* 238, 794-814.
- [25] Dyrkacz G. R, Libby R. D, Hamilton G. A (1976) Trivalent copper as a probable intermediate in the reaction catalyzed by galactose oxidase. *J. Am. Chem. Soc.* 98, 626-628
- [26] Hamilton G. A, Adolf P. K, de Jersey J, DuBois G. C, Dyrkacz G. R, Libby, R. D (1978) Trivalent copper, superoxide, and galactose oxidase. *J. Am. Chem. Soc.* 100, 1899-1912.
- [27] Clark K, Penner-Hahn J. E, Whittaker M. M, Whittaker J. W (1990) Oxidation-state assignments for galactose oxidase complexes from x-ray absorption spectroscopy. Evidence for copper(II) in the active enzyme. *J. Am. Chem. Soc.* 112, 6433-6435.
- [28] McGlashen M. L, Eads D. D, Spiro T. G, Whittaker J. W (1995) Resonance Raman Spectroscopy of Galactose Oxidase: A New Interpretation Based on Model Compound Free Radical Spectra. *J. Phys. Chem.* 99, 4918-4922.
- [29] Jazdzewski B. A, Tolman, W. B (2000) Understanding the Copper-Phenoxyl Radical Array in Galactose Oxidase: Contributions From Synthetic Modeling Studies. *Coord. Chem. Rev.* 200-202, 633-685.
- [30] Thomas F. (2007) Ten Years of a Biomimetic Approach to the Copper(II) Radical Site of Galactose Oxidase. *Eur. J. Inorg. Chem.* 2379-2404.
- [31] Shimazaki Y, Yamauchi O. (2011) Recent Advances in Metal-Phenoxyl Radical Chemistry. *Indian J. Chem.* 50A, 383-394.
- [32] Shimazaki. Y, Huth, S, Hirota, S, Yamauchi O (2000) Chemical Approach to the Cu(II)-Phenoxyl Radical Site in Galactose Oxidase: Dependence of the Radical Stability on N-Donor Properties. *Bull. Chem. Soc. Jpn.* 73, 1187-1195.
- [33] Shimazaki, Y, Huth, S, Odani, A, Yamauchi, O (2000) A Structure Model for Galactose Oxidase Active Site and Counteranion-Dependent Phenoxyl Radical Formation by Disproportionation. *Angew. Chem. Int. Ed.* 39, 1666-1669

- [34] Shimazaki, Y, Huth, S, Hirota, S, Yamauchi, O (2002) Studies on Galactose Oxidase Active Site Model Complexes: Effects of Ring Substituents on Cu(II)-Phenoxy Radical Formation. *Inorg. Chim. Acta*, 331, 168-177.
- [35] Pratt, R. C, Stack, T. D. P (2003) Intramolecular Charge Transfer and Biomimetic Reaction Kinetics in Galactose Oxidase Model Complexes. *J. Am. Chem. Soc.* 125, 8716-8717.
- [36] Pratt, R. C, Stack, T. D. P (2005) Mechanistic Insights from Reactions between Copper(II)-Phenoxy Complexes and Substrates with Activated C-H Bonds. *Inorg. Chem.* 44, 2367-2375.
- [37] Jacobsen, E. N (2000) Asymmetric Catalysis of Epoxide Ring-Opening Reactions. *Acc. Chem. Res.* 33, 421.
- [38] Pfeiffer P, Brietg E, Lubbe E, Tsumaki T (1933) Tricyclische orthokondensierte Nebenvale nzringe. *Justus Liebigs Ann. Chem.* 503, 84.
- [39] Shimazaki, Y, Tani, F, Fukui, K, Naruta, Y, Yamauchi, O (2003) One-electron Oxidized Nickel(II)-Di(salicylidene)diamine Complexes: Temperature Dependent Tautomerism between Ni(III)-Phenolate and Ni(II)-Phenoxy Radical States. *J. Am. Chem. Soc.* 125, 10512-10513.
- [40] Shimazaki, Y, Yajima, T, Tani, F, Karasawa, S, Fukui, K, Naruta, Y, Yamauchi, O (2007) Syntheses and Electronic Structures of One-Electron-Oxidized Group 10 Metal(II)-(Disalicylidene)diamine Complexes (Metal = Ni, Pd, Pt). *J. Am. Chem. Soc.* 129, 2559-2568.
- [41] Storr T, Wasinger E. C, Pratt R. C, Stack T. D. P (2007) The Geometric and Electronic Structure of a One-Electron-Oxidized Ni(II) bis-(salicylidene)diamine Complex. *Angew. Chem. Int. Ed.* 46, 5198-5201.
- [42] Shimazaki, Y, Stack, T. D. P, Storr, T (2009) Detailed Evaluation of the Geometric and Electronic Structures of One-Electron Oxidized Group 10 (Ni, Pd, and Pt) Metal(II)-(Disalicylidene)diamine Complexes. *Inorg. Chem.* 48, 8383-8392.
- [43] Shimazaki, Y, Arai, N, Dunn, T. J, Yajima, T, Tani, F, Ramogida, C. F, Storr, T. (2011) Influence of the chelate effect on the electronic structure of one-electron oxidized group 10 metal(II)-(disalicylidene)diamine complexes. *Dalton Trans.* 40, 2469.
- [44] Orio M, Jarjays O, Kanso H, Philouze C, Neese F, Thomas F (2010) X-Ray Structures of Copper(II) and Nickel(II) Radical Salen Complexes: The Preference of Galactose Oxidase for Copper(II). *Angew. Chem. Int. Ed.* 49, 4989-4992.
- [45] Storr T, Verma P, Pratt R. C, Wasinger E. C, Shimazaki Y, Stack T. D. P. (2008) Defining the Electronic and Geometric Structure of One-Electron Oxidized Copper-Bis-phenoxide Complexes. *J. Am. Chem. Soc.* 130, 15448-15459.
- [46] Thomas F, Jarjays O, Duboc C, Philouze C, Saint-Aman E, Pierre J.-L (2004) Intramolecularly hydrogen-bonded versus copper(II) coordinated mono- and bis-phenoxyl radicals. *Dalton Trans.* 2662-2669.
- [47] Kochem A, Jarjays O, Baptiste B, Philouze C, Vezin H, Tsukidate K, Tani F, Orio M, Shimazaki Y, Thomas F (2012) One-Electron Oxidized Copper(II) Salophen Complexes: Phenoxy versus Diiminobenzene Radical Species. *Chem. Eur. J.* 18, 1068-1072.
- [48] Whiteoak C. J, Salassa G, Kleij A. W (2012) Recent Advances with π -conjugated Salen Systems. *Chem. Soc. Rev.* 41, 622-631.

- [49] Dunn T. J, Ramogida C. F, Simmonds C, Paterson A, Wong E. W. Y, Chiang L, Shimazaki Y, Storr T (2011) Non-Innocent Ligand Behavior of a Bimetallic Ni Schiff-Base Complex Containing a Bridging Catecholate. *Inorg. Chem.* 50, 6746-6755.
- [50] Glaser T, Heidemeier M, Fröhlich R, Hildebrandt P, Bothe E, Bill E (2005) Trinuclear Nickel Complexes with Triplesalen Ligands: Simultaneous Occurrence of Mixed Valence and Valence Tautomerism in the Oxidized Species. *Inorg. Chem.* 44, 5467-5482.
- [51] Bordwell F. G, Cheng J. P. (1991) Substituent effects on stabilities of phenoxyl radicals and the acidities of phenoxyl radical cations. *J. Am. Chem. Soc.* 113, 1736-1743.
- [52] Webster R. D (2003) In situ electrochemical-ATR-FTIR spectroscopic studies on solution phase 2,4,6-tri-substituted phenoxyl radicals. *Electrochem. Commun.* 5, 6-11.
- [53] Thomas F (2010) Metal Coordinated Phenoxyl Radicals. in: Hicks, R. G, editor. *Stable Radicals: Fundamental and Applied Aspects of Odd-Electron Compounds*. Wiley, pp. 281-316.
- [54] Freire C, Castro B (1998) Spectroscopic characterisation of electrogenerated nickel(III) species. Complexes with N2O2 Schiff-base ligands derived from salicylaldehyde. *J. Chem. Soc., Dalton Trans.* 1491-1498.
- [55] Bag B, Mondal N, Rosair G, Mitra S (2000) The first thermally-stable singly oxo-bridged dinuclear Ni(III) complex. *Chem. Commun.* 1729-1730.
- [56] Barnard C. T. J, Russel M. J. H (1987) Palladium and Platinum. in: Wilkinson G, Gillard R. D, McCleverty J. A editors. *Comprehensive Coordination Chemistry*; Pergamon, Oxford, Vol. 5.
- [57] Connelly N. G, Geiger W. E (1996) Chemical Redox Agents for Organometallic Chemistry. *Chem. Rev.* 96, 877-910.
- [58] Emsley, J (1998) *The Elements*, 3rd Edition, Oxford, Oxford University Press.
- [59] Iwasawa, Y (1995) *X-Ray Absorption Fine Structure for Catalysts Surfaces*. London, World Scientific Publishing.
- [60] Müller J, Weyhermüller T, Bill E, Hildebrandt P, Ould-Moussa L, Glaser T, Wieghardt K (1998) Why Does the Active Form of Galactose Oxidase Possess a Diamagnetic Ground State? *Angew. Chem. Int. Ed.* 37, 616-619.
- [61] Kahn O. (1985) Dinuclear Complexes with Predictable Magnetic Properties. *Angew. Chem., Int. Ed. Engl.* 24, 834-850.
- [62] Chong D. P (1995) *Recent Advances in Density Functional Methods*. Singapore, World Scientific.
- [63] Rotthaus O, Jarjayes O, Thomas F, Philouze C, Del Valle C. P, Saint-Aman E, Pierre J. -L (2006) Fine Tuning of the Oxidation Locus, and Electron Transfer, in Nickel Complexes of Pro-Radical Ligands. *Chem. Eur. J.* 12, 2293-2302.
- [64] Rotthaus O, Thomas F, Jarjayes O, Philouze C, Saint-Aman E, Pierre J. -L (2006) Valence Tautomerism in Octahedral and Square-Planar Phenoxyl-Nickel(II) Complexes: Are Imino Nitrogen Atoms Good Friends? *Chem. Eur. J.* 12, 6953-6962.
- [65] Robin M. B, Day P (1967) Mixed-valence chemistry: a survey and classification. *Adv. Inorg. Chem. Radiochem.* 10, 247-422.